

# Multistable localized states in highly photonic polariton rings with a quasiperiodic modulation

Andrei V. Nikitin and Dmitry A. Zezyulin

*School of Physics and Engineering, ITMO University, St. Petersburg 197101, Russia*

We present a theoretical study of an exciton-polariton annular microcavity with an additional quasiperiodic structure along the ring which is implemented in the form of a bicosine dependence. We demonstrate that for a sufficiently strong quasiperiodic modulation, the microcavity features a sharp mobility edge separating a cluster of localized states from the rest of the spectrum consisting of states extended over the whole ring. Localized modes can be excited using a resonant pump whose topological charge determines the phase distribution of excited patterns. Repulsive polariton interactions make the resonance peaks distinctively asymmetric and enable the formation of multistable states which feature the attractor-like dynamical behavior and hysteresis. We also demonstrate that the localized states can be realized in a biannular cavity that consists of two rings, each having periodic modulation, such that the periods of two modulations are different.

## I. INTRODUCTION

Cavity polaritons are composite light-matter quasiparticles that emerge in a planar semiconductor microcavity operating in the so-called strong-coupling regime<sup>1,2</sup>. From their photonic component, cavity polaritons have macroscopically large coherence length, while the excitonic fraction enables strong polariton-polariton interactions. Another peculiarity of exciton-polaritons is their inherently nonequilibrium nature due to the photon leakage from the cavity. A quasistationary regime can be achieved when losses are compensated with a resonant or nonresonant pump. Exciton-polaritons can be confined and controlled by external potentials of various shapes. State-of-the-art nanotechnology provides a variety of polariton trapping techniques and various means for controllable energy landscape engineering<sup>3</sup>. In particular, polaritons can be confined in nonsimply-connected, i.e., ring- or multiring-shaped geometries<sup>4,5</sup> which facilitate the manifestation of the superfluid nature of polariton condensates<sup>6</sup> through the formation of vortex states, persistent circular currents, and rotating patterns, see e.g. Refs.<sup>7–15</sup>. In addition, exciton-polaritons undergo condensation at relatively high temperatures as compared to Bose condensates of cold atoms. Combination of these properties makes exciton-polaritons an ideal platform for studies of quantum collective phenomena in an environment where nonlinear and nonequilibrium effects play a prominent role.

A remarkable example of such a phenomenon is the spatial localization in incommensurate lattices. While this behavior is known for more than 40 years, at least since the pioneering work of Aubry and André (AA)<sup>16</sup>, quasicrystalline systems and a host of associated physical phenomena — such as the existence of the mobility edge, ‘metal-insulator transition’, and the fractal energy spectrum — continue to attract steadily growing attention in various areas of physics. For cavity polaritons, the localization in quasiperiodic structures has been experimentally observed in layered systems based on the one-dimensional polaritonic wires structured in

the form that interpolates between the AA and Fibonacci sequences<sup>17,18</sup>. In the experiments reported on in Ref.<sup>18</sup>, the polaritonic wires were excited with a weak non-resonant cw laser, and spatially extended and localized states were identified using the spectrally resolved photoluminescence signal either in real and in  $k$  space. In the meantime, the theoretical treatment of exciton-polaritons that undergo the localization in quasiperiodic landscapes has mostly been limited by the linear and conservative limit, and a complete account of the strong polariton nonlinearity and resonant pump has not yet been performed.

The main goal of the present work is to explore the effect of resonant pump and nonlinearity on the formation and stability of localized states in a structured microcavity. We treat the problem using the so-called approximant path which replaces the quasiperiodic system with a long-periodic one<sup>19–21</sup>. This transformation suggests considering the system under the periodic boundary conditions, and therefore the annular geometry becomes the most natural one. We model a polariton condensate confined in an annular-shaped cavity which has an additional quasiperiodic structuring approximated using a bicosine landscape. It is assumed that the condensate has a high photonic fraction, which makes the phonon-assisted energy relaxation less efficient. We show that this system can feature a sharp mobility edge that separates delocalized and localized states. A peculiarity of the adopted approach is that the number of localized states can be controlled by the chosen rational approximation (at least, in a certain range of parameters). Another representative feature of the annular geometry is the possibility to excite localized states using a vortical ring-shaped resonant pump which produces a number of closely spaced resonances. Vorticity of the pump can be used to control the phase portrait of localized patterns. In the nonlinear regime, the resonant peaks become strongly asymmetric, which results in multistable localized states coexisting at the same the pump frequency. Dynamical simulations reveal that each unstable state dynamically switches to its stable counterpart situated in the upper branch of the

multistable resonance curve. The existence of localized states is illustrated for two configurations: the first one corresponds to a single ring with an additional biperiodic modulation, and the second one is a biannular structure, where the two rings have modulations with different periods.

The organization of the paper is as follows. In Sec. II we introduce the adopted theoretical model. In Sec. III we describe localized states in the linear and conservative regime (i.e., when the resonant pump and losses are neglected). In Sec. III we present the results on the resonant excitation of linear and nonlinear states and demonstrate that in the latter case the multistability takes place. Section III is devoted to the excitation of out-of-phase localized states using a resonant pump with a properly chosen vorticity. Section VI provides a conclusion and a short outlook.

## II. MODEL

A well-known possibility to realize the quasiperiodicity corresponds to a bichromatic potential comprising two periodic potentials of incommensurate periods. While the AA model implements such a situation in a tight-binding approximation, the simplest example of a spatially-continuous one-dimensional quasiperiodic potential is a bicosine landscape  $V_0[\cos z + \cos(\varphi z)]$ , where  $\varphi$  is an irrational number,  $z \in \mathbb{R}$  is a spatial coordinate, and  $V_0$  is the amplitude. Complete understanding of even such a relatively simple potential can be an overwhelmingly complex task, see e.g.<sup>19,20,22–28</sup>. One of possible approaches relies on the use of a rational approximation  $\varphi \approx M/N$ , where  $M \gg 1$  and  $N \gg 1$  are coprime integers. This approach proceeds by replacing the quasiperiodic potential by the following one:

$$V_{\text{1D}}(z) = V_0[\cos z + \cos(Mz/N)]. \quad (1)$$

The latter potential is *periodic* with the period equal to  $2\pi N$ , and therefore it cannot support truly localized states, i.e., eigenstates that satisfy the zero boundary conditions at the infinity. However the concept of localization can be nevertheless introduced by considering Bloch waves that are strongly localized within the unit cell  $[-\pi N, \pi N)$ . Such an *approximant path*<sup>21</sup> allows one to reach the physics of quasicrystals using the well-developed Fourier-Floquet-Bloch machinery and, moreover, enables the concept of topological quasicrystals<sup>21</sup>. In particular, topological invariants of the resulting minibands (such as Chern numbers or Zak phases) can be connected to the spatial distribution of the localized states<sup>29</sup>.

The transformation from a quasiperiodic system to a large-periodic one suggests considering the latter one under the periodic boundary conditions. Therefore, the annular geometry becomes the most natural one for such a system. In this study, we consider a system of exciton-polaritons formed by cavity photons coupled to quantum well excitons. We assume that polaritons are confined in

a structured ring-shaped cavity and their dynamics can be described by a single classical field for lower-branch polaritons. Then the dynamics can be modelled using the coherently driven Gross-Pitaevskii equation<sup>6</sup> (GPE)

$$i\psi_t = \left[ -\frac{1}{2}(\partial_x^2 + \partial_y^2) + V + |\psi|^2 - i\gamma \right] \psi + h(r)e^{im\theta - i\epsilon t}. \quad (2)$$

Equation (2) is written in normalized units: for the effective polariton mass  $m \approx 10^{-34}$  kg and the unit length  $\ell \approx 1 \mu\text{m}$ , the adopted normalization corresponds to the time unit  $m\ell^2/\hbar \approx 1$  ps and the energy unit  $\hbar/(m\ell^2) \approx 0.7$  meV. Function  $h(r)$  describes the spatial modulation of resonant pump (hereafter  $r \geq 0$  and  $\theta \in [-\pi, \pi)$  are the polar coordinates). We assume that  $h(r)$  is characterized by the maximal amplitude  $h_0$  and has annular shape with the same radius  $r_0$  as that of the ring-shaped microcavity, and the width of the annular pump is much larger than that of the cavity ring, i.e., the intensity of the pump beam is almost uniform over the cavity. Integer  $m$  is the topological charge of the pump beam. The nonlinear term  $\propto |\psi|^2$  corresponds to polariton interactions. Small coefficient  $\gamma$  accounts for polariton losses (we use model value  $\gamma \approx 0.02$ ). Function  $V$  describes the landscape of the confining potential. To specify its shape, we for a moment return to the  $2\pi N$  one-dimensional periodic potential (1) and map its unit cell  $[-\pi N, \pi N)$  to the period of the polar angle, i.e., to  $[-\pi, \pi)$ . A simple transformation  $\theta = z/N$  leads to the following bicosine dependence:  $V_0[\cos(N\theta) + \cos(M\theta)]$ . We therefore use the following landscape for potential  $V$  in Eq. (2):

$$V(r, \theta) = V_R(r)[1 + \delta(\cos(N\theta) + \cos(M\theta))]. \quad (3)$$

Here function  $V_R(r)$  models the uniform ring potential:  $V_R(r) = -V_0 e^{-(r-r_0)^2/w_0^2}$ , where  $V_0$ ,  $r_0$ , and  $w_0$  are positive parameters that tune depth of the annular potential, its radius, and width, respectively. Coefficient  $\delta \in (0, 1)$  is the strength of the quasiperiodic modulation in units of the average depth  $V_0$ . In recent experiments, the energy landscape gradient along the ring has been realized by the variation of the thickness of the microcavity<sup>30</sup>. Several proposals on the implementation of a modulated annular cavities have been recently outlined in Ref.<sup>31</sup>. In particular, a circularly distributed modulation can be realized with a structured optical mask imaged onto the sample<sup>32,33</sup>.

We note that the coherently driven GPE equation (2) is a simplified model which is generally valid only if the Rabi frequency is large as compared to other relevant energy scales<sup>6</sup>. In addition, Eq. (2) disregards the polariton energy relaxation that is known to be prominent in certain polaritonic systems<sup>34–37</sup>. Nevertheless this model still can be useful to predict the very existence of localized states. The description provided by Eq. (2) is expected to be more accurate for highly photonic condensates where the phonon-assisted energy relaxation becomes less efficient. An equation of mathematically sim-

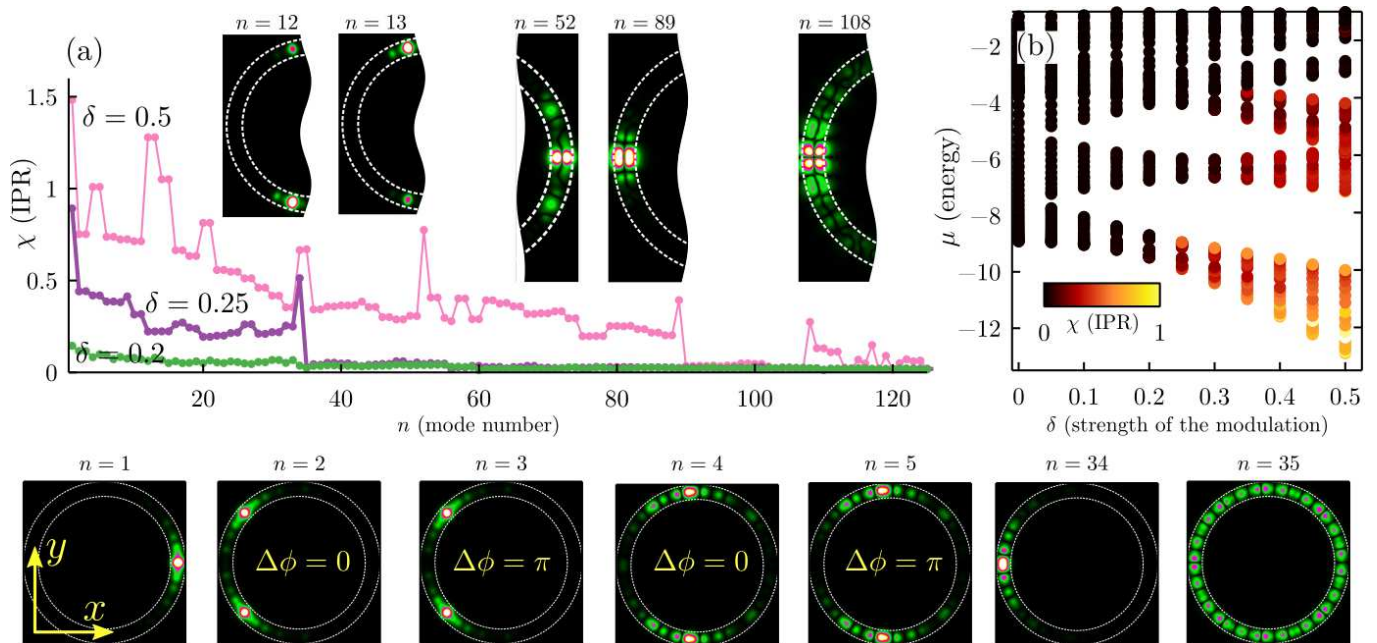


FIG. 1: (a) IPR  $\chi$  for 125 lowest linear eigenstates (enumerated with index  $n = 1, 2, \dots$ ) for three different strengths of the quasiperiodic modulation:  $\delta = 0.2, 0.25$ , and  $0.5$ . (b) Energy  $E$  vs.  $\delta$  for lowest eigenvalues. Different colors correspond to different values of the IPR. Seven lowest panels: moduli distribution  $|\psi(x, y)|$  for several representative eigenstates for  $\delta = 0.25$ . Labels  $\Delta\phi = 0$  and  $\Delta\phi = \pi$  correspond to in-phase and out-of-phase double-peaked states, respectively. Upper diagrams: several moduli distributions for  $\delta = 0.5$ : a pair of asymmetric localized states ( $n = 12, 13$ ), two double states ( $n = 52, 89$ ), and a quadruple state ( $n = 108$ ); for compactness of the figure, only part of the ring is shown for these states. In this picture radius  $r_0 = 10$ , squared meanwidth  $w_0^2 = 0.5$ , average depth  $V_0 = 12$ ;  $M = 55$ ,  $N = 34$ .

ilar structure (known as the Lugiato-Lefever equation<sup>38</sup>) is used to model light dynamics in planar cavities filled with a nonlinear Kerr medium. Recent experiments (see e.g.<sup>39,40</sup>) report on the possibility of patterning a ring-shaped optical microresonator with implementing a photonic crystal or a multifrequency photonic crystal along the microring. The results of our study can be relevant in this subfield as well.

### III. LINEAR LOCALIZED STATES IN THE CONSERVATIVE REGIME

The spectrum of stationary eigenstates  $\psi = e^{-i\mu t}u(x, y)$  has been found numerically from the two-dimensional eigenvalue problem obtained from Eq. (2) in the regime where nonlinearity, losses  $\gamma$ , and pump  $h(r)$  are switched off. To model the potential, we have used  $M = 55$  and  $N = 34$  in Eq. (3). These two subsequent Fibonacci numbers correspond to a rational approximation of the golden ratio  $M/N \approx \varphi = (1 + \sqrt{5})/2$ . To quantify the localization of eigenmodes, we use the inverse participation ratio (IPR) defined as (see e.g.<sup>18,28</sup>)

$$\chi = \frac{\iint_{-\infty}^{\infty} |\psi|^4 dx dy}{(\iint_{-\infty}^{\infty} |\psi|^2 dx dy)^2}. \quad (4)$$

In Fig. 1(a) we present IPRs computed for 125 lowest-energy states for three different values of the modulation strength  $\delta$ . For  $\delta \lesssim 0.2$  all states are delocalized or only weakly localized, i.e., extended along the ring (with IPRs below 0.15). In this case a distinctive mobility edge, i.e., a sharp boundary between localized and delocalized states, cannot be found in the spectrum. However, at  $\delta = 0.25$  we observe that there are exactly 34 localized states (with IPRs  $\gtrsim 0.2$ ) which are situated at the bottom of the spectrum and are sharply distinguished from the delocalized modes (compare panels  $n = 1, 2, \dots, 34$  with  $n = 35$  in the lowest row of Fig. 1). Thus, similar to the earlier studies where the rational approximation was used for one-dimensional quasiperiodic potentials (see in particular<sup>29,43</sup>), the exact number of localized states can be controlled by the choice of the adopted rational approximation. In the one-dimensional quasiperiodic potential (1) this behavior can be explained by the fact that each spectral band of the  $2\pi$ -periodic potential associated with the first cosine splits into  $N$  *minibands* in the spectrum of the full  $2\pi N$ -periodic potential comprising both cosines. From the pseudocolor diagram in Fig. 1(b) we observe that for  $\delta = 0.25$  there is a relatively large gap between the energies of localized and delocalized states (again, this agrees with the earlier results for one-dimensional lattices<sup>28</sup>). A closer inspection of localized states shows that there are two single-peak states (corresponding to  $n = 1$  and  $n = 34$ ),

where the location of the peak corresponds to  $\theta = 0$  and  $\theta = \pi$ , respectively. Due to the symmetry of the potential with respect to the angular reversal  $\theta \rightarrow -\theta$ , other localized states consist of pairs of in-phase and out-of-phase two-peaked states having close energies, with the phase difference between the peaks equal to  $\Delta\phi = 0$  and  $\Delta\phi = \pi$ , respectively, see panels  $n = 3, 4$  and  $n = 4, 5$  in the lowest row of Fig. 3. For stronger modulation (such as  $\delta = 0.5$ ), the picture becomes more complex. In particular, there appear pairs of asymmetric states which are degenerate, i.e., have equal energies (notice that localized states of this type are impossible in the strictly one-dimensional geometry subject to the zero boundary conditions due to the well-known fact that the one-dimensional Schrödinger equation cannot have double eigenvalues associated with localized eigenstates<sup>41</sup>). Moreover, a sufficiently strong modulation enables localization of more complex states that belong to upper polariton subbands and feature a distinct structure along the radial coordinate (see e.g. double and quadruple states displayed in panels  $n = 52, 89, 108$  in Fig. 1). Similar states with complex transverse distribution have been detected experimentally in quasi-1D polariton wires<sup>18</sup>. As a result of the excitation of the upper subbands, the strongly modulated potential supports more localized states and can have multiple mobility edges corresponding to the *reentrant* localization transition, see the interval  $n = 100 \dots 120$  for  $\delta = 0.5$  in Fig. 1(a). The first transition from localized to delocalized states corresponds to  $n = 89$  which is another Fibonacci number.

Concluding the discussion of localization in the linear and conservative regime, we notice that the excitation of localized states is also possible in a *biannular* structure, where each ring has a periodic modulation, and the periods are different for both rings. The corresponding potential landscape can be represented as

$$V = V_R(r)[1 + \delta_M \cos(M\theta)] + V_R(r - \Delta r)[1 + \delta_N \cos(N(\theta + \theta_0))], \quad (5)$$

where  $\Delta r > 0$  is the difference between the ring radii,  $\theta_0$  is the angular shift between the two rings, and  $\delta_{M,N}$  are the modulation strengths for larger ( $M$ ) and smaller ( $N$ ) rings. Several examples of localized states found in such a structure are displayed in Fig. 2.

#### IV. RESONANCES, MULTISTABILITY, AND HYSTERESIS-LIKE BEHAVIOR

Next, we proceed to the localized states in the presence of the resonant pump and polariton nonlinearity. We focus on the cavity with the single structured ring described by potential (3). When the pump and losses are switched on (in the so far linear system), the localized states produce a picture with multiple coexisting resonances which is shown in Fig. 3(a) as a dependence

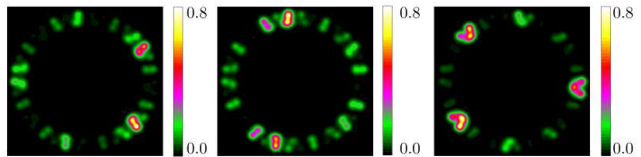


FIG. 2: Examples of localised states in the biannular potential that consists of two structured rings, see Eq. (5). Here  $N = 21$ ,  $M = 34$ ,  $\delta_M = 0.45$  and  $\delta_N = 0.35$ . Radii of the rings are  $r_0 = 10$  and  $r_0 - \Delta r = 8.6$ .

of maximal amplitude of the excited pattern on the pump frequency  $\varepsilon$ . The spectrum of IPRs (shown in the inset) features a similar resonant structure. The total number of resonant peaks in Fig. 3(a) is less than the number of localized states that can be found in the conservative regime. This is due to the fact the zero-charged resonant pump cannot excite out-of-phase states (this issue will be discussed below in Sec. V).

In the linear system, each resonant peak is symmetric with respect to sufficiently small left and right detunings from the frequency corresponding to the center of the peak, where the local maximum of the excited amplitude is achieved. Therefore no more than one linear state can be resonantly excited at each frequency. However, when the nonlinearity is taken into account, the resonant peaks become distinctively asymmetric, as illustrated in Fig. 3(b) for two different pump amplitudes  $h_0$ , compare left and right vertical axes in this figure. Only a part of the picture corresponding to the resonances at relatively small frequencies is shown in Fig. 3(b). Since the degree of asymmetry of resonance peaks strengthens with the increase of  $h_0$ , for a sufficiently large pump amplitude two or more nonlinear states coexist at the same value of the pump frequency  $\varepsilon$ , which can result in bi- or multistability. To illustrate the stability properties of localized states, we present the dynamical modelling results for nine nonlinear states coexisting at the pump strength  $h_0 = 0.006$  and frequency  $\varepsilon = -10.59$  [marked with the vertical dotted line in Fig. 3(b)]. This figure indicates that there are five multistable states at the chosen frequency which are always situated at upper branches of tilted resonant peaks (see the evolutions corresponding to solid lines in Fig. 4). Other four states are unstable, and each unstable mode dynamically switches into the stable mode at the corresponding upper branch. Therefore stable states feature the attractor-like behavior.

The results plotted in the inset in Fig. 3(b) indicate that for stronger pump strengths the IPRs of the excited states tend to decrease. This behavior can be explained by the nonlinearity-induced hybridization between several localized states, which results in the excitation of patterns composed of several pairs of bright spots. Three examples of such hybridized states are shown in the bottom row of Fig. 4. Solutions with larger maximal amplitude contain more bright peaks than those with small

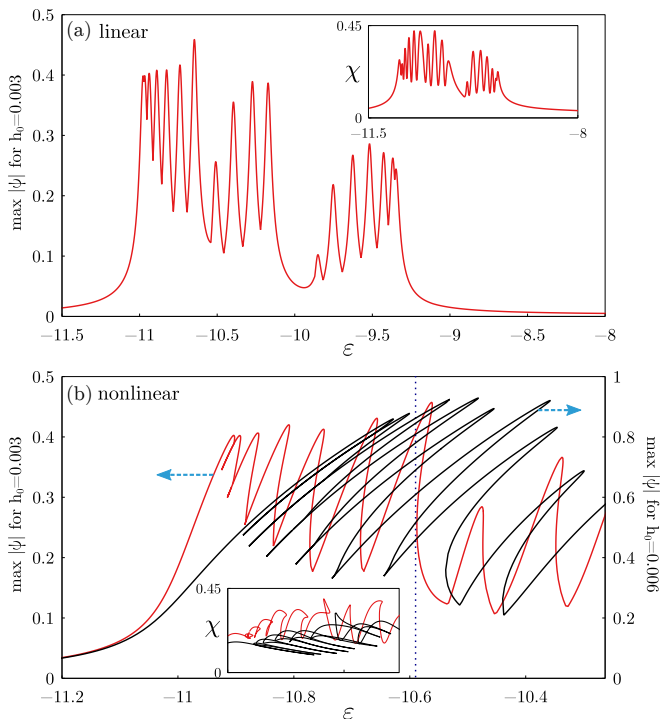


FIG. 3: (a): Maximal amplitude  $\max_{(x,y)} |\psi|$  for linear states excited by the resonant pump with maximal amplitude  $h_0 = 0.003$ . (b): Resonances in the nonlinear regime for two values of  $h_0$  ( $h_0 = 0.003$  and  $h_0 = 0.006$  corresponding to the left and to the right vertical axis, respectively); notice that in this panel only part of all resonances is displayed. The insets show IPRs  $\chi$ . In this figure, the pump is zero-charged, i.e.,  $m = 0$ .

amplitudes. This trend in general agrees with the repulsive character of the polariton interactions which are expected to promote the delocalization of strongly nonlinear high-amplitude states.

The nonlinear response of the system can also be probed using the adiabatic increase of the pump intensity as illustrated in Fig. 5. In the regime of weak pump, the excited amplitude grows linearly with the pump strength. However, the further increase of the pump strength eventually leads to the deviation from the linear growth law and triggers a cascade of jumps from low-amplitude to high-amplitude stable states (in Fig. 5, these jumps are separated by spiky transients). The increase of the pump amplitude  $h_0$  is accompanied by the general decay of the IPR  $\chi$ , which results from the excitation of additional bright spots in the high-amplitude solution [compare plots (a) and (b) in the lower row of Fig. 5]. The multi-stable nature of the system manifests in a hysteresis-like behavior<sup>42</sup>: when the pump amplitude is switched from increasing to decreasing, the system undergoes a different evolution (see small arrows in Fig. 5 that highlight different paths followed by the system as the pump amplitude  $h_0$  increases and decreases). The upper branch of the amplitude curve in Fig. 5 corresponds to the lower

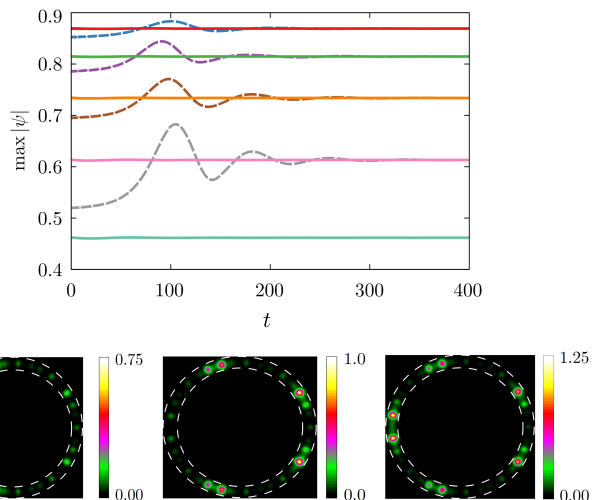


FIG. 4: Upper panel shows temporal dynamics of maximal amplitude  $\max_{(x,y)} |\psi|$  for nine nonlinear states coexisting at the pump frequency  $\varepsilon = -10.59$  for pump amplitude  $h_0 = 0.006$  [see dotted vertical line in Fig. 3(b)]. Solid and dashed curves correspond to the evolution of stable and unstable states, respectively. Three lower panels show moduli  $|\psi|$  for the three stable solutions with largest IPRs.

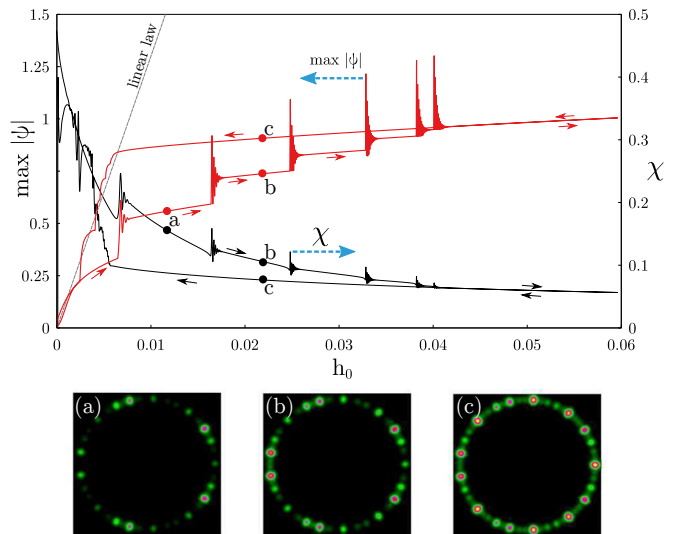


FIG. 5: The upper panel shows the evolution of the maximal amplitude (left vertical axis) and IPR (right vertical axis) as the pump amplitude changes in time (at first, increases from  $h_0 \approx 0$  to  $h_0 \approx 0.06$  and then decreases from  $h_0 \approx 0.06$  to  $h_0 \approx 0$ ). Small arrows correspond to the increase of time and highlight the hysteresis-like response. Points (a,b,c) in the upper panel correspond to the solutions shown in the lower row. The results are computed using the numerical integration of Eq. (2) in the nonlinear regime, at the zero-charged pump at frequency  $\varepsilon = -10.647$ .

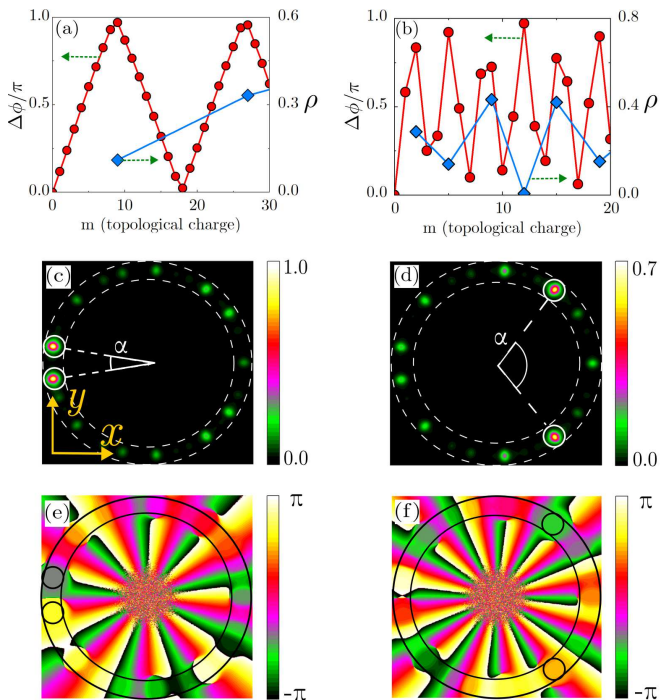


FIG. 6: (a,b) Phase difference  $\Delta\phi$  (in units of  $\pi$ ) and roundoff distance  $\rho$  as functions of topological charge  $m$  for two different out-of-phase states with  $\alpha \approx 20^\circ$  (a) and  $\alpha \approx 105^\circ$  (b); panels (c,d) and (e,f) show modulus and phase distributions of out-of-phase states excited with vortical resonance pump with  $m = 9$  (c,e) and  $m = 12$  (d,f). This figure corresponds to the linear regime.

branch of the IPR curve.

## V. EXCITATION OF OUT-OF-PHASE STATES WITH VORTICAL PUMP

As noted above in Sec. III, the spectrum of linear localized states includes multiple pairs of in-phase and out-of-phase two-peaked modes which are situated at relatively close energies. The zero-charged resonant pump (i.e. that with  $m = 0$ ) dictates that the phase of the excited pattern is uniform along the ring and therefore it cannot excite out-of-phase modes. However, the latter can be excited using a vortical pump with a properly chosen topological charge  $m$ . Let  $\alpha \in (0, \pi)$  be the angle formed by the two radii connecting the center of the ring and the two out-of-phase spots in a given solution (see illustration in Fig. 6). The phase difference between these peaks is equal to  $\Delta\phi_1 = (2q + 1)\pi$ , where  $q = 0, 1, \dots$  is an unknown integer. At the same time, the pump beam with topological charge equal to  $m$  induces the phase incursion equal to  $\Delta\phi_2 = m\alpha$  over the angle  $\alpha$ . The “optimal” situation for the excitation of the purest out-of-phase state would correspond to the exact equality  $\Delta\phi_1 = \Delta\phi_2$ . However, since  $m$  is integer, this equality, generically speaking, can be satisfied only approximately. To find a topological charge which

corresponds to the purest out-of-phase mode, we introduce an auxiliary quantity  $\mu_q = (2q + 1)\pi/\alpha$  and for each  $q$  measure the distance between  $\mu_q$  and the closest integer by introducing  $\rho_q = |\mu_q - [\mu_q]|$ , where  $[\mu]$  means round towards nearest integer. The optimal situation takes place if for some  $q$  one has  $\rho_q = 0$ . Then the out-of-phase state can be excited with the topological charge  $m = \mu_q$ . To check this prediction, we perform the direct simulation of excited states for different topological charges (limiting the consideration by  $m$  ranging from 0 to 30) and measure the phase difference  $\Delta\phi$  between the two peaks. In Fig. 6(a,b) we juxtapose the dependencies  $\Delta\phi/\pi$  vs.  $m$  and  $\rho_q$  vs.  $[\mu_q]$  for two different out-of-phase states. These results confirm that the purest out-of-phase states with  $\Delta\phi \approx \pi$  are indeed excited by topological charges that correspond to small values of  $\rho_q$ . It should be emphasized that, since different out-of-phase states correspond to different angles  $\alpha$ , the optimal topological charges are also generically different.

## VI. CONCLUSION

We have presented a theoretical study for localization of exciton-polaritons in annular microcavities which have an additional quasiperiodic modulation implemented as a bicosine dependence. We have started with the localization diagram in the linear and conservative regime, demonstrated that the cavity can feature a sharp mobility edge, and classified the localized states. Then it has been shown that the localized patterns can be excited using a resonant pump and feature distinctive nonlinear behavior which results in multistability, i.e., in the coexistence of several dynamically stable states at the same frequency of resonant pumping. The complexity of the nonlinear resonances diagram, i.e., the number of coexisting stable and unstable branches, can be controlled by changing the intensity of the incident pump beam. The multistable states dynamically behave as attractors, and unstable states dynamically switch to their stable counterparts from upper branches of tilted resonance peaks. A nonmonotonic change of the pump amplitude results in a hysteresis, i.e., the nonequivalence of paths followed by the system as the pump amplitude increases and decreases. Most of the localized states exist in the form of in-phase and out-of-phase dipoles, and the latter one can be excited by tuning the topological charge of the vortical pump.

We expect that our results will promote further research of nonlinear effects for exciton-localized polariton states that form in quasicrystalline and disordered media. One relevant direction of future work is related to a thorough analysis of polarization effects that can be taken into account in the form of the TE-TM splitting. The pseudospin degree of freedom may considerably enrich the behavior of localized states. Its effect can be especially interesting if considered together with an external magnetic field applied to the microcavity. Another rele-

vant issue is the excitation of localized state using an incoherent, off-resonant pumping scheme which is expected to enable more complex dynamical behavior, such as the nonlinear symmetry-breaking or dynamical oscillations between different stable localized modes, similar to the multimode dynamics recently explored for atomic Bose-Einstein condensates in one-dimensional bichromatic optical lattices<sup>43</sup>. It would also be interesting to study the role of the repulsive polariton interaction in the context of a finite-temperature phase transition between fluid and insulator that was theoretically predicted for disordered

weakly interacting bosons in Ref.<sup>44</sup>.

### Acknowledgments

The authors are grateful to Igor Chestnov and Alexey Yulin for valuable discussions. This work was supported by the Ministry of Science and Higher Education of Russian Federation (“goszadanie no. 2019-1246”), and by “Priority 2030 Academic Leadership Program”.

- 
- <sup>1</sup> H. Deng, H. Haug, and Y. Yamamoto, Exciton-polariton Bose-Einstein condensation, *Rev. Mod. Phys.* **82**, 1489 (2010).
- <sup>2</sup> D. D. Solnyshkov, G. Malpuech, P. St-Jean, S. Ravets, J. Bloch, and A. Amo, Microcavity polaritons for topological photonics, *Opt. Mater. Express* **11**, 1119–1142 (2021).
- <sup>3</sup> C. Schneider, K. Winkler, M. D. Fraser, M. Kamp, Y. Yamamoto, E. A. Ostrovskaya, and S. Höfling, Exciton-polariton trapping and potential landscape engineering, *Rep. Prog. Phys.* **80**, 016503 (2017).
- <sup>4</sup> A. Dreismann, P. Cristofolini, R. Balili, G. Christmann, F. Pinsker, N. G. Berloff, Z. Hatzopoulos, P. G. Savvidis, and J. J. Baumberg, Coupled counterrotating polariton condensates in optically defined annular potentials, *Proc. Natl. Acad. Sci. USA* **111**, 8770 (2014).
- <sup>5</sup> G. Liu, D. W. Snoke, A. Daley, L. N. Pfeiffer, and K. West, A new type of half-quantum circulation in a macroscopic polariton spinor ring condensate, *Proc. Natl. Acad. Sci. USA* **112**, 2676 (2015).
- <sup>6</sup> I. Carusotto and C. Ciuti, Quantum fluids of light, *Rev. Mod. Phys.* **85**, 299 (2013).
- <sup>7</sup> G. Li, M. D. Fraser, A. Yakimenko, and E. A. Ostrovskaya, Stability of persistent currents in open dissipative quantum fluids, *Phys. Rev. B* **91**, 184518 (2015).
- <sup>8</sup> Y. V. Kartashov and D. A. Zezyulin, Rotating patterns in polariton condensates in ring-shaped potentials under a bichromatic pump, *Opt. Lett.* **44**, 4805 (2019).
- <sup>9</sup> F. Barkhausen, S. Schumacher, and X. Ma, Multistable circular currents of polariton condensates trapped in ring potentials, *Opt. Lett.* **45**, 1192 (2020).
- <sup>10</sup> A. V. Yulin, A. V. Nalitov, and I. A. Shelykh, Spinning polariton vortices with magnetic field, *Phys. Rev. B* **101**, 104308 (2020).
- <sup>11</sup> F. Barkhausen, M. Pukrop, S. Schumacher, and X. Ma, Structuring coflowing and counterflowing currents of polariton condensates in concentric ring-shaped and elliptical potentials, *Phys. Rev. B* **103**, 075305 (2021).
- <sup>12</sup> A. K. Bochyn and A. V. Nalitov, Nonequilibrium polariton condensation in biannular optically induced traps, *Opt. Mater. Express* **13**, 295 (2023).
- <sup>13</sup> I. Gnusov, S. Harrison, S. Alyatkin, K. Sitnik, J. Topfer, H. Sigurdsson, P. G. Lagoudakis, Quantum vortex formation in the “rotating bucket” experiment with polariton condensates, *Sci. Adv.* **9**, eadd1299 (2023).
- <sup>14</sup> Y. del Valle-Inclan Redondo, C. Schneider, S. Klemmt, S. Höfling, S. Tarucha, and M. D. Fraser, Optically Driven Rotation of Exciton-Polariton Condensates, *Nano Lett.* **23**, 4564 (2023).
- <sup>15</sup> V. Lukoshkin, E. Sedov, V. Kalevich, Z. Hatzopoulos, P. G. Savvidis, and A. Kavokin, Steady state oscillations of circular currents in concentric polariton condensates, *Sci. Rep.* **13**, 4607 (2023).
- <sup>16</sup> S. Aubry and G. André, Analyticity breaking and Anderson localization in incommensurate lattices, *Ann. Isr. Phys. Soc.* **3**, 133 (1980).
- <sup>17</sup> D. Tanese, E. Gurevich, F. Baboux, T. Jacqmin, A. Lemaître, E. Galopin, I. Sagnes, A. Amo, J. Bloch, and E. Akkermans, Fractal Energy Spectrum of a Polariton Gas in a Fibonacci Quasiperiodic Potential, *Phys. Rev. Lett.* **112**, 146404 (2014).
- <sup>18</sup> V. Goblot, A. Štrkalj, N. Pernet, J. L. Lado, C. Dorow, A. Lemaître, L. Le Gratiet, A. Harouri, I. Sagnes, S. Ravets, A. Amo, J. Bloch, and O. Zilberberg, Emergence of criticality through a cascade of delocalization transitions in quasiperiodic chains, *Nature Phys.* **16**, 832–836 (2020).
- <sup>19</sup> R. B. Diener, G. A. Georgakis, J. Zhong, M. Raizen, and Qian Niu, Transition between extended and localized states in a one-dimensional incommensurate optical lattice, *Phys. Rev. A* **64**, 033416 (2001).
- <sup>20</sup> X. Li, X. Li, and S. Das Sarma, Mobility edges in one-dimensional bichromatic incommensurate potentials, *Phys. Rev. B* **96**, 085119 (2017).
- <sup>21</sup> O. Zilberberg, Topology in quasicrystals, *Opt. Mater. Express* **11**, 1143–1157 (2021).
- <sup>22</sup> J. Frölich, T. Spencer, and P. Wittwer, Localization for a Class of One Dimensional Quasi-Periodic Schrödinger Operators, *Commun. Math. Phys.* **132**, 5–25 (1990).
- <sup>23</sup> H. Broer and C. Simó, Hill’s equation with quasi-periodic forcing: resonance tongues, instability pockets and global phenomena, *Bol. Soc. Bras. Mat.* **29**, 253 (1998).
- <sup>24</sup> J. L. Cohen, B. Dubetsky, and P. R. Berman, Quasiperiodic Fresnel atom optics, focusing, and the quasi-Talbot effect, *Phys. Rev. A* **60**, 3982 (1999).
- <sup>25</sup> D. J. Boers, B. Goedeke, D. Hinrichs, and M. Holthaus, Mobility edges in bichromatic optical lattices, *Phys. Rev. A* **75**, 063404 (2007).
- <sup>26</sup> M. Modugno, Exponential localization in one-dimensional quasi-periodic optical lattices, *New J. Phys.* **11**, 033023 (2009).
- <sup>27</sup> J. Biddle, B. Wang, D. J. Priour, Jr., and S. Das Sarma, Localization in one-dimensional incommensurate lattices beyond the Aubry-André model, *Phys. Rev. A* **80**, 021603(R) (2009).
- <sup>28</sup> H. Yao, H. Khoudli, L. Bresque, and L. Sanchez-

- Palencia, Critical Behavior and Fractality in Shallow One-Dimensional Quasiperiodic Potentials, *Phys. Rev. Lett.* **123**, 070405 (2019).
- <sup>29</sup> D. A. Zezyulin and V. V. Konotop, Localization of ultracold atoms in Zeeman lattices with incommensurate spin-orbit coupling, *Phys. Rev. A* **105**, 063323 (2022).
- <sup>30</sup> S. Mukherjee, V. K. Kozin, A. V. Nalitov, I. A. Shelykh, Z. Sun, D. M. Myers, B. Ozden, J. Beaumariage, M. Steger, L. N. Pfeiffer, K. West, and D. W. Snoke, Dynamics of spin polarization in tilted polariton rings, *Phys. Rev. B* **103**, 165306 (2021).
- <sup>31</sup> I. Chestnov, Y. G. Rubo, A. Nalitov, and A. Kavokin, Pseudoconservative dynamics of coupled polariton condensates, *Phys. Rev. Research* **3**, 033187 (2021).
- <sup>32</sup> R. Dall, M. D. Fraser, A. S. Desyatnikov, G. Li, S. Brodbeck, M. Kamp, C. Schneider, S. Höfling, and E. A. Ostrovskaya, Creation of Orbital Angular Momentum States with Chiral Polaritonic Lenses, *Phys. Rev. Lett.* **113**, 200404 (2014).
- <sup>33</sup> M. Wurdack, E. Estrecho, S. Todd, C. Schneider, A. G. Truscott, and E. A. Ostrovskaya, Enhancing Ground-State Population and Macroscopic Coherence of Room-Temperature  $\text{WS}_2$  Polaritons through Engineered Confinement, *Phys. Rev. Lett.* **129**, 147402 (2022).
- <sup>34</sup> M. Wouters, T. C. H. Liew, and V. Savona, Energy relaxation in one-dimensional polariton condensates, *Phys. Rev. B* **82**, 245315 (2010).
- <sup>35</sup> M. Wouters, Energy relaxation in the mean-field description of polariton condensates, *New J. Phys.* **14**, 075020 (2012).
- <sup>36</sup> I. G. Savenko, T. C. H. Liew, and I. A. Shelykh, Stochastic Gross-Pitaevskii Equation for the Dynamical Thermalization of Bose-Einstein Condensates, *Phys. Rev. Lett.* **110**, 127402 (2013).
- <sup>37</sup> K. Winkler, O. A. Egorov, I. G. Savenko, X. Ma, E. Estrecho, T. Gao, S. Müller, M. Kamp, T. C. H. Liew, E. A. Ostrovskaya, S. Höfling, and C. Schneider, Collective state transitions of exciton-polaritons loaded into a periodic potential, *Phys. Rev. B* **93**, 121303(R) (2016).
- <sup>38</sup> L. A. Lugiato, F. Prati, M. L. Gorodetsky, and T. Kippenberg, From the Lugiato-Lefever equation to microresonator-based soliton Kerr frequency combs, *Phil. Trans. R. Soc. A* **376**, 20180113 (2018).
- <sup>39</sup> E. Lucas, S.-P. Yu, T. C. Briles, D. R. Carlson, and S. B. Papp, Spontaneous pulse formation in edgeless photonic crystal resonators, *Nat. Photonics* **15**, 461-467 (2021).
- <sup>40</sup> G. Moille, X. Lu, J. Stone, D. Westly, K. Srinivasan, Fourier synthesis dispersion engineering of photonic crystal microrings for broadband frequency combs, *Commun. Phys.* **6**, 144 (2023).
- <sup>41</sup> L. D. Landau and E. M. Lifshitz, *Quantum Mechanics. Nonrelativistic Theory. Second Edition*, p. 60 (Pergamon Press, Oxford 1965).
- <sup>42</sup> N. N. Rosanov, *Spatial Hysteresis and Optical Patterns* (Springer-Verlag Berlin Heidelberg 2002).
- <sup>43</sup> H. C. Prates, D. A. Zezyulin, and V. V. Konotop, Bose-Einstein condensates in quasiperiodic lattices: Bosonic Josephson junction, self-trapping, and multimode dynamics, *Phys. Rev. Research* **4**, 033219 (2022).
- <sup>44</sup> I. L. Aleiner, B. L. Altshuler, and G. V. Shlyapnikov, A finite-temperature phase transition for disordered weakly interacting bosons in one dimension, *Nature Phys.* **6**, 900 (2010).